International Journal of Scientific & Engineering Research, Volume 4, Issue 12, December-2013
ISSN 2229-5518

Countermeasure Detection in the Two-Color Pulsed Infrared seekers Using Pulse Number

S. Y. Alchekh Yasin, A. R.Erfanian, M. R. Mosavi, A. Mohammadi

Abstract—One of the important parts of the infrared seeker is the counter countermeasure part. Seeking in a field of view with the existence of jammers is not simple and needs effective algorithms. In this paper, several methods of the detection in a crossed array trachers (CAT) seeker will be designed, simulated and evaluated. One of these methods, which is detecting the flare using the pulses number relatively to an adaptive threshold, is a novel one.

.

Index Terms—Infrared Seeker, Counter Countermeasure, Crossed Array Detectors (CAT), Adaptive Threshold, Field of view (FOV).

1 Introduction

THE IR counter-countermeasure (IRCCM) built into advanced missiles have two parts. The first part is detecting the existence or the appearance of the flares in the seeker field of view (FOV) and activating the process for overcoming these jammers; sometime this part is called switch part. The second part is applying the IRCCM algorithms to overcome the jammers effect on the seeking process; sometime this part is called response part [1-2]. The jammers is a flare or an active jammer. The missile must detect the jammer existence or appearance before initiating a counter proccess.

When a flare is detected by the seeker in an advanced IR missile, the seeker will switch on the IRCCM response to reject the flare . Both the switch and response must operate properly to successfully reject the flare and continue tracking the target. There are many different switch and response techniques available to the missile designers, thus a device that is capable of decoying one advanced IR missile type may be totally ineffective against another advanced IR missile.

Detecting the existence or the appearance of the flares in a short time is a critical task, as increasing the required time of detection gives the flare the required time to push the real target out of the effective work region of the FOV, and as a result missing the real target [2-5].

Detecting the existence of an active jammer is a more advanced process than that of the flare. As mostly, the active jammer is already switched on.

In this paper, it is stated several methods for detecting the flares in the FOV of a crossed array detectors seeker (CAT) or a four crossed slits reticle seeker. Increasing in the pulses number in one spin period is an indication of a new target in the FOV, so this criterion will be discussed in several ways. One of the important methods is detecting using the pulses number relatively to an adaptive threshold. Counting the pulses needs to define a reference level up to which the pulse appearance is counted, and making this threshold an adaptive one which changes each period up to the level of the information signals is the main idea of this novel method. Finally, a comparison of the methods and its main principles will be stated.

All the modeling and simulation tasks and processes will be designed and developed using the MATLAB® tools and packages.

The structure of the crossed ship reticle or the crossed four slits reticle (Actually it is equivalent to a reticle with four crossed array detectors CAT), which is a stationary reticle type, will be stated with the design parameters. This type employs a fixed reticle, with radius Ra and N=4 transparent sectors or slits, and a slightly tilted rotating mirror or lens (with spinning frequency fm) to sweep the Target Image Spot (TIS) along a circular path on the reticle Target Imaging Circle (TIC) with constant radius (RN), as shown in Fig. 1,2,3. The distance of the non-concentric TIC centre and its phase relatively to the reticle centre define the position of the target in the FOV [6-10].

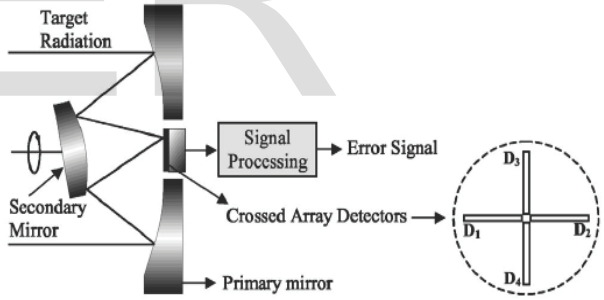

Fig.1. The cross ship reticle.

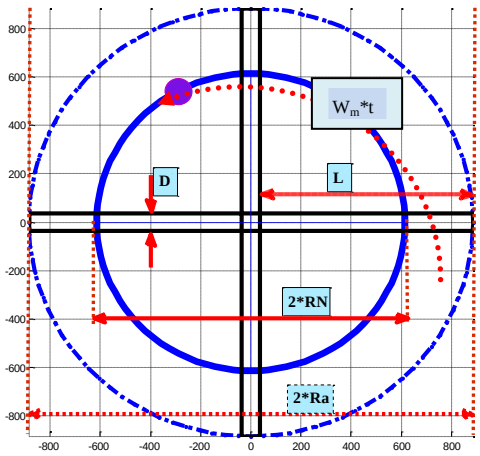

Fig. 2. Design parameters of a CAT reticle (D,L, Ra, RN).

IJSER © 2013
http://www.ijser.org

In Fig 2 the defined parameters:

1. D: the spoke width or the detector width (pixel).
2. L: the spoke length or the detector length (pixel).
3. Ra: the reticle radius (FOV radius) (pixel).
4. RN: the target imaging circle (TIC) (pixel).

In this study, theses parameters take the following values: (D=70, L=850, RN=615, Ra=885) unit or pixel. When the TIC is not concentrate with the reticle, which means that the target position is not on the centre of the FOV, the imaging circle centre (or the target position) parameters (aT(t), β0 (t)) can be defined.

The used reticle model takes the reticle parameters (D, L, Ra, RN) as inputs and gives the output signal up to the target position parameters, such the coordination in the Field Of View (FOV). For modelling the two-color seeker, a model of a detector with variant band limits, [λmin1, λmax1] for the (M band) in mid IR region and [λmin2, λmax2] for the (N band) in near IR region. The detectors outputs (M1T,M2T,M1J,M2J) will forms the two color channels by combining with the reticle outputs [11-14]. An as result, six signals will be produced using the final used model:

1. Y1(ch1) and Y2(ch2) are the main channel and the secondary channel signals.
2. Yt1 and Yt2 are the signals resulting from the existence of the real target in the FOV in the two channels respectively.
3. Yj1 and Yj2 are the signals resulting from the existence of a flare in the FOV in the two channels respectively.

2 Seeker Modeling Relations

Every object over 0K emits IR radiation depending on its temperature and its spectral distribution is given as a function of temperature by Planck's law as follows :

$$W(T,\lambda) = \frac{2.\pi.h.c^2}{\lambda^5.\left(e^{\left(\frac{h.c}{\lambda.k.T}\right)}-1\right)} = \frac{c_1}{\lambda^5.\left(e^{\left(\frac{c_2}{\lambda.T}\right)}-1\right)} \quad (1)$$

where c1 and c2 are the first and second radiation constants, and k, h, λ, and T are the Boltzman's constant, the Planck's constant, the wavelength, and absolute temperature. The IR normalized spectral distributions depend strongly on temperature; the spectrum peak moves to shorter wavelength as the temperature rises, as shown in figure 3.

The output of the detector on the M band which is defined by [λmin1, λmax1] is given by:

$$D_1(t) = D_{[\lambda min1,\lambda max1]}(T(t)) = \int_{\lambda min1}^{\lambda max1} W(T(t),\lambda).d\lambda \quad (2)$$

Similarly, the output of the detector on the N band which is defined by [λmin2, λmax2] is given by:

$$D_2(t) = D_{[\lambda min2,\lambda max2]}(T(t)) = \int_{\lambda min2}^{\lambda max2} W(T(t),\lambda).d\lambda \quad (3)$$

As a result, the outputs of two-color detectors in the existence of a target and a jammer are:

$$D_{1T}(T(t)) = D_1(T_T(t)),\ D_{2T}(T(t)) = D_2(T_T(t)) \quad (4)$$

$$D_{1J}(T(t)) = D_1\left(T_J(t)\right),\ D_{2J}(T(t)) = D_2\left(T_J(t)\right) \quad (5)$$

Or

$$D_{1T}(T[n]) = D_1(T_T[n]),\ D_{2T}(T[n]) = D_2(T[n]) \quad (6)$$

$$D_{1J}(T[n]) = D_1(T_J[n]),\ D_{2J}(T[n]) = D_2(T_J[n]) \quad (7)$$

On each detector all IR radiations pass through the reticle and become modulated signals; therefore, these modulated signals will be integrated on the surface of the detector with weights related to the temperature and surface of each target or flare. So the channels signals can be written as:

$$Y(ch1) = Rad(T_T,S_T) * m_T[n] + Rad(T_J,S_J) * m_J[n] \quad (8)$$

$$Y(ch1) = H_1(S_T) * D_{1T}[n] * m_T[n] + H_1(S_J) * D_{1J}[n] * m_J[n] \quad (9)$$

$$Y(ch2) = H_2(S_T) * D_{2T}[n] * m_T[n] + H_2(S_J) * D_{2J}[n] m_J[n] \quad (10)$$

Where m_J, m_T are the modulations resulting from the reticle on the target and the jammer signals respectively.

Actually, H1 and H2 can be generalized to include all the external parameters distributed from the target or the flare to the detectors. Therefore, by taking into accounts that (H1=H2) is the same for the same IR object and by normalizing relativly to the target, the relations can be rewrite:

$$Y(ch1) = Y_{1T}[n] + Y_{1J}[n] \quad , \quad Y(ch2) = Y_{2T}[n] + Y_{2J}[n] \quad (11)$$

Where

$$Y_{1T}[n] = \gamma_T * D_{1T}[n] * m_T[n]$$

$$Y_{2T}[n] = \gamma_T * D_{2T}[n] * m_T[n]$$

$$Y_{1J}[n] = \gamma_J * D_{1J}[n] * m_J[n]$$

$$Y_{2J}[n] = \gamma_J * D_{2J}[n] * m_J[n] \quad (12)$$

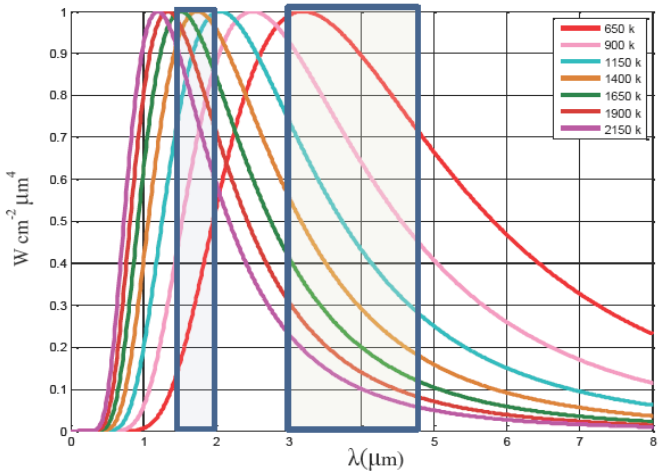

Fig.3. Normalized spectral distributions of IR sources. The shaded spectral regions represent the N and M bands.

IJSER © 2013
http://www.ijser.org

3 JAMMER MODELING

The flare is modeled by designing a flare temperature profile generator and a flare position generator. The flare temperature profile determines the profile of the flare signal amplitude, so the profile of the main channel amplitude with time. The output temperature is given by the following equations:

$$T_F = T_{max} * \begin{cases} 0 & (t < t_0) \text{ or } (T_f < t) \\ 1 - e^{-\frac{t-t_0}{T_r}} & t_0 \le t < t_0 + T_1 \\ e^{-\frac{(t-T_r-t_0)}{T_b}} & t_0 + T_1 \le t \le t_0 + T_f \end{cases} \quad (12)$$

where t0 is the launch instant, Tf is the flare life duration, Tr is the rise time constant, T1 is the rise duration, Tb is the burn time constant, and Tmax is the maximum temperature. This temperature TF variable will be the flare temperature input of the seeker model [14].

The flare movement generator, as shown in Fig 4, determines the flare position in the FOV with time, the main parameters of that are the movement of the flare in the space and the distance from the missile to the flare [15-16]. Taking into account the FOV angle is usually ±1degee, the FOV space will be a disc with a radius of (R*17)m where R(km) is the distance from the missile and the flare. In addition to that, the initial speed or the launch speed of the flare is [20-30]m/s. As result of that, the flare movement scenario in the FOV can be determined. Up to the practices previous ranges, and taking into accounts that reticle radius is (885 pixls) the speed of the flares in the FOV in the simulation in the range [500,2500] pixel/s, which means that the flare remains in the FOV [0.35,1.5]s.

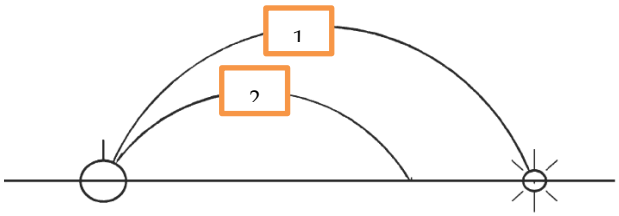

Fig. 4. The movement profile of the flare in the space.

For an active jammer it has to define [6-8]:

$$M(x,y) = \Delta(n_1, N_1) + \Delta(n_2, N_2) + \Delta(n_3, N_3) + \Delta(n_4, N_4) \quad (14)$$

$$n_i = P_i(x,y), N_i = W_i(x,y) \dots \dots i = 1,2,3,4 \quad (15)$$

$$m_T(x_T, y_T, r_T) = M(x_T, y_T) * \emptyset(x_T, y_T, r_T) \quad (16)$$

$$\emptyset(x_T, y_T, r_T \cong 0) = 1 \quad (17)$$

$$m_J(x_J, y_J) = m_J(x_T, r_T) = M(x_T, y_T) * \varphi(t) \quad (18)$$

$$\varphi(t) = [0.5 + 0.5 * \cos(2 * \pi * f_J * t + \theta_J(t))] \quad (19)$$

So:

$$m_J(x_J, y_J) = m_J(x_T, r_T) = M(x_T, y_T) * [0.5 + 0.5 * \cos(2 * \pi * f_J * t + \theta_J(t))] \quad (20)$$

Where fj , θj are the jammer signal frequency and phase respectively. And as a result the seeker signals will be:

$$Y(ch1) = \gamma_T * D_{1T}[n] * M(x_T, y_T) * \emptyset(x_T, y_T, r_T) + \gamma_J * D_{1J}[n] * M(x_T, y_T) * \varphi(t) \quad (21)$$

$$Y(ch1) = M(x_T, y_T) * \{\gamma_T * D_{1T}[n] * \emptyset(x_T, y_T, r_T) + \gamma_J * D_{1J}[n] * \varphi(t)\} \quad (22)$$

$$Y(ch1) = M(x_T, y_T) * A * \{\emptyset(x_T, y_T, r_T) + \eta * [0.5 + 0.5 * \cos(2 * \pi * f_J * t + \theta_J(t))]\} \quad (23)$$

With:

$$\max\|M(x_T, y_T)\| = \max\|\emptyset(x_T, y_T, r_T)\| = \max\|\varphi(t)\| = 1 ,$$

$$\eta[n] = \frac{\|Y_{1J}[n]\|}{\|Y_{1T}[n]\|} > 1 \quad (24)$$

For a certain target and a certain active jammer:

$$\eta = \text{Const}(S_T, S_J) * \text{Const}(T_T, T_J) = \frac{\gamma_J}{\gamma_T} . \frac{D_{1J}}{D_{1T}} = \eta_1 * \eta_2 \quad (25)$$

Figure 5 shows the following case:

1. Target
   - temperature: 850k. so $D_{1T} = 1.07$, $\gamma_T = 2$.
   - dx = dy = 1000 pixel/s .
2. Jammer
   - temperature: 1500k. so $D_{1T} = 7.9$, $\gamma_J = 0.3$.
   - fJ=18000Hz, Phase=0 degree.
3. So : $\eta = \frac{\gamma_J}{\gamma_T} . \frac{D_{1J}}{D_{1T}} = \eta_1(0.15) * \eta_2(7.36) = 1.1$

The effect of the jammer depends on the process of dialing with the case of number of pulses more than 4. Clearly the jammer will be effect when it can produce pulses more than 4 as shown in Fig 5 and Fig 6.

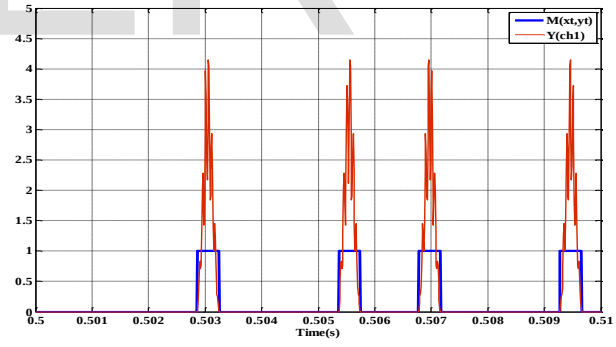

(a)

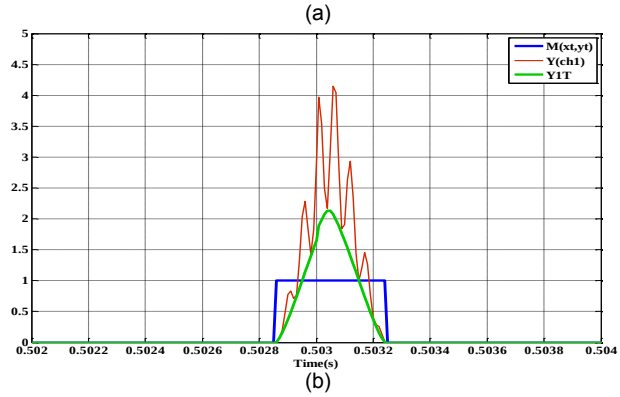

(b)

Fig.5.Seeker signals in the case of a target (temperature: 850k. so $D_{1T} = 1.07$, $\gamma_T = 2$, dx = dy = 1000 pixel/s) and a jammer (temperature: 1500k. so $D_{1J} = 7.36$, $\gamma_J = 0.3$, fj=18000Hz).

IJSER © 2013
http://www.ijser.org

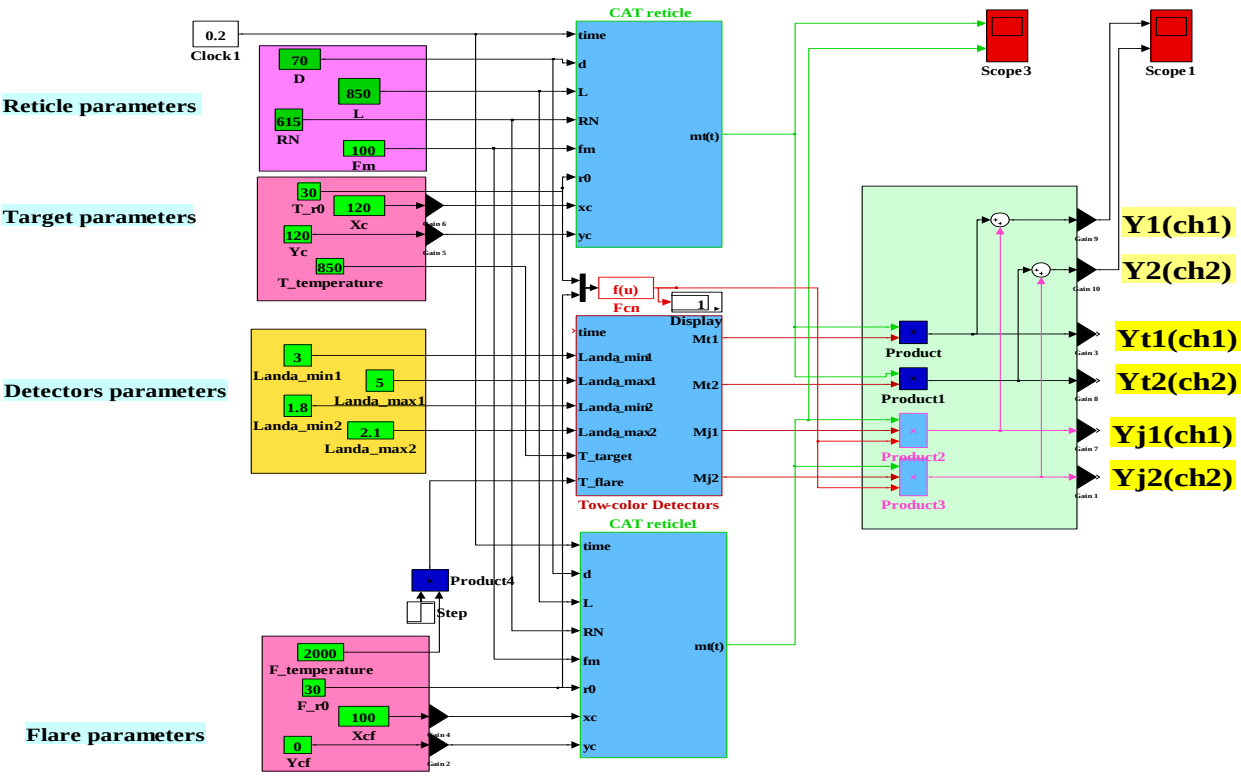

Fig. 6. The final model with the inputs (reticle parameters, detectors parameters, target parameters, and flare parameters) and the outputs (Y1(ch1), Y2(ch2), Ref=YT1, YT2, Yj1 , Yj2).

4 Detection Flare Using the Pulses Number Relatively to a Constant Threshold.

The pulse is counted when the signal of the main channel exceeds a certain threshold and return lower than it, and the pulse width will be the interval between these two instants. In the general case, each target produces at most four pulses in each spinning period, four if the target position locates in the effective work region which means that the TIC intersects the four slits; less than four when the intersection with one or more slits is missed. So increasing the pulses number more than four that indicates to the existence of other IR source. So in this method the pulses number produced in the previous spinning period will be the detection parameter [14-16].

For explaining this method, several parameters have to be defined. On the period]t-Tm,t], or digitally on]n-Nm,n]:

1. Mn-Nm(thr1): the number of the pulses exist in this spinning period]n-Nm,n] relatively to the threshold thr1.

For simplifying:

1. Mthr1 = Mn-Nm(thr1).
2. M=Mconstant.

Firstly, the pulse number (M) for a flare with the following parameters are gotten and drawing in the Fig 7:

1. (Tlanuch=0.2s, Trise=0.25s, Tf=3.5s, Tb=4, Tmax=2000k, Tmin=850k).
2. speed={500,1000,1500,2000}pixel/s.
3. Tr= {0.01, 0.05, 0.1, 0.2, 0.25, 0.3}.

And as a result the data are resumed in the table 12. From this table:

1. The detection using M is independent of the temperature profile while it depends mainly on the movement of the flare.
2. It is clear that M detects the instant of the separation of the pulses produced by the target and those produced by the flare.
3. M is inverse proportional to the speed of the flare.

The flowchart of using the condition (M>5) in the CAT seeker is stated in Fig 8.

TABLE 1

THE REQUIRED TIME FOR DETECTION (TREQ (S)) USING (M>4) CONDITION FOR SEVERAL TR AND SPEEDS.

Speed (pixel/s)	Tr	0.01	0.05	0.1	0.2	0.3
500		0.23	0.24	0.24	0.23	0.23
1000		0.12	0.12	0.12	0.12	0.12
1500		0.08	0.08	0.08	0.08	0.08
2000		0.07	0.07	0.06	0.06	0.07

IJSER © 2013
http://www.ijser.org

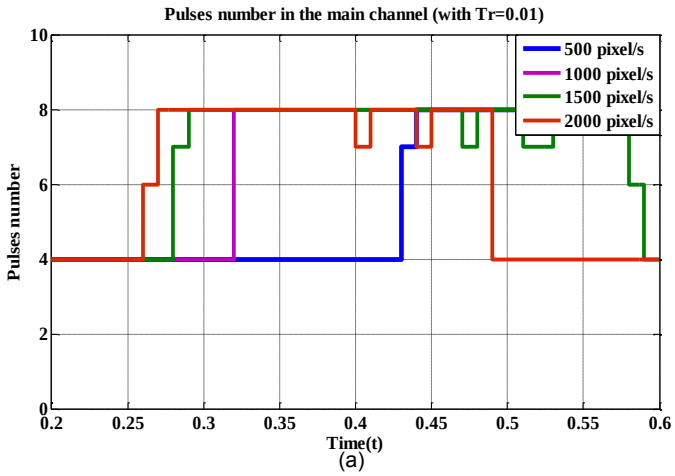

(a)

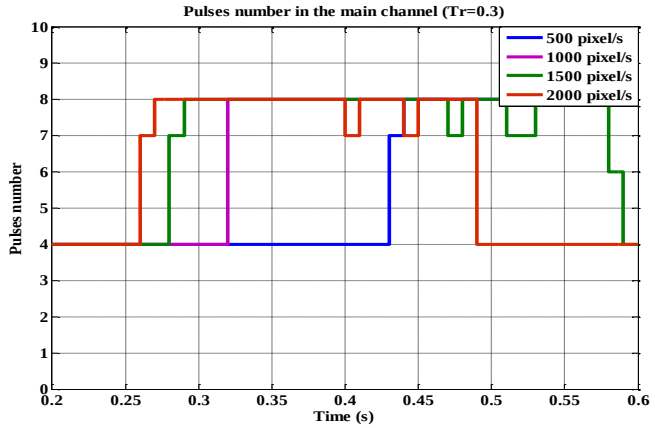

(b)

Fig.7. Pulses number (M) in the main channel for a Flare (Tlanuch=0.2s, Trise=0.25s, Tf=3.5s, Tb=4, Tmax=2000k, Tmin=850k), speed={500,1000,1500,200} pixel/s: (a) Tr=0.01 (b) Tr=0.3

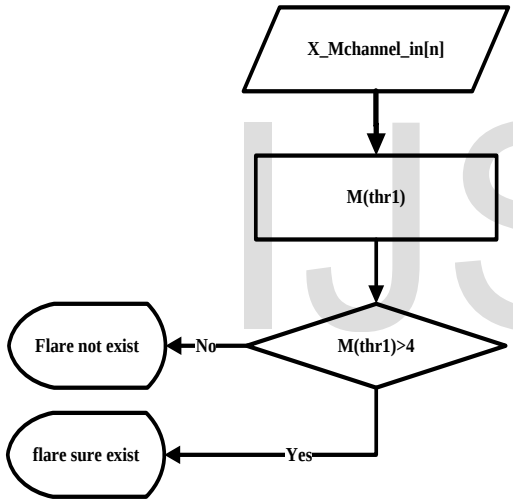

Fig.8. The flowchart of the flare detection using the pulses number (M).

5 Detection Flare Using the Pulses Number Relatively to an Adaptive Threshold.

These conceptions will be used:

1. The first phase: the duration between the flare launch and the instant when the pulses of the flare and those of the target are separated in the information signal up to certain threshold (thr1).
2. The second phase : the phase after the separation.
3. Separating instant tth1 : the instant separating the two phases up to the threshold (thr1).

In the general case, each target produces at most four pulses in each spinning period. So increasing the pulses number more than four that indicates to the existence of another IR source. So in the previous method the pulses number produced in the previous spinning period relative to a constant threshold (M(thr1)) was the detection parameter. It is clear that this method detects the instant of the separation (tth1). In this novel method an adaptive threshold is defined to detect the appearance of new pulses before the separation instant (tth1).

As show in Fig 9, if the threshold is chosen with bigger value (thr2>thr1) the separation will be detected earlier (tth2<tth1). On other hand, if the threshold is so big (thr3>>thr1) it may lose the detection, and this losing is related to both the temperature profile and the movement of the flare. In addition to that, the threshold which is appropriate in some cases, like thr2, it may be not in other cases as show in Fig 9.

This novel method suggests an adaptive threshold (thr_a) which will be related to the pulses maximum in the previous spinning period A[1] with a parameter Q1 as the following relation:

$$thr\_a = Q1 * A[1] \quad (22)$$

This is clarified in Fig 10.The rang of Q1 is [0.25,0.65] to avoid the false alarm resulting from the noise superposed on the signal. So our goal is finding the appropriate value of the parameter Q1.

Firstly, the pulses number M(thr_a) for a flare with the following parameters are gotten:

(Tlanuch=0.2s, Trise=0.25s, Tf=3.5s, Tb=4, Tmax=2000k, Tmin=850k).

speed={500, 1500}pixel/s.

Tr= {0.01, 0.10, 0.20}.

And the results are resumed in the tables (2-3) and some cases are shown in Fig 11. From the tables above it is clear that the value (Q1 = 0.35) is the appropriate one and this is verified in the table 4. The improvement of the required time for detection which this method provides is clarified by a comparison between the table 1 and the table 4. The flowchart of using the condition (M(th_a)>4) in the CAT seeker is stated in Fig 12. This method will be notes as (MA).

IJSER © 2013
http://www.ijser.org

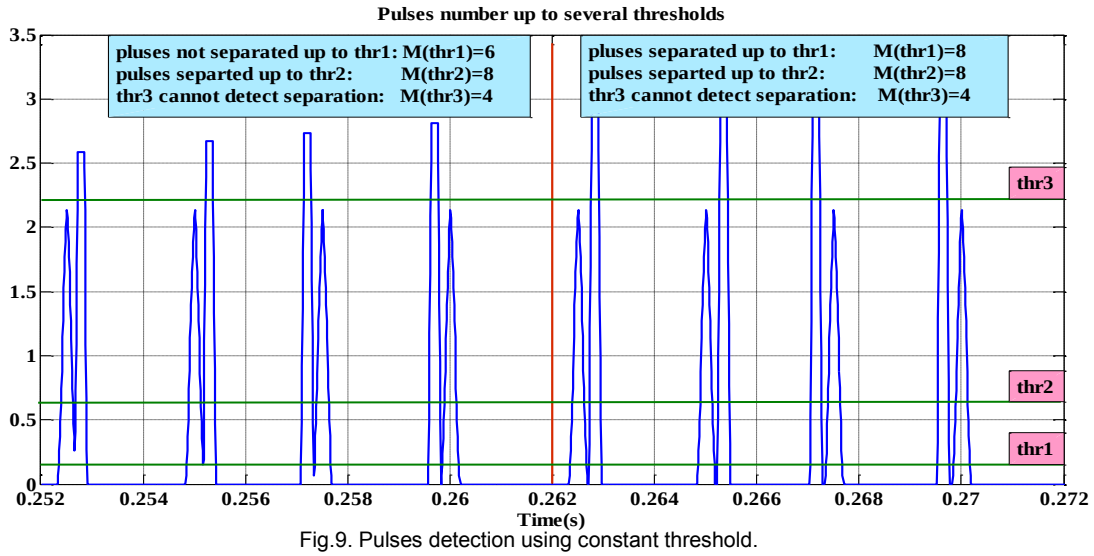

Fig.9. Pulses detection using constant threshold.

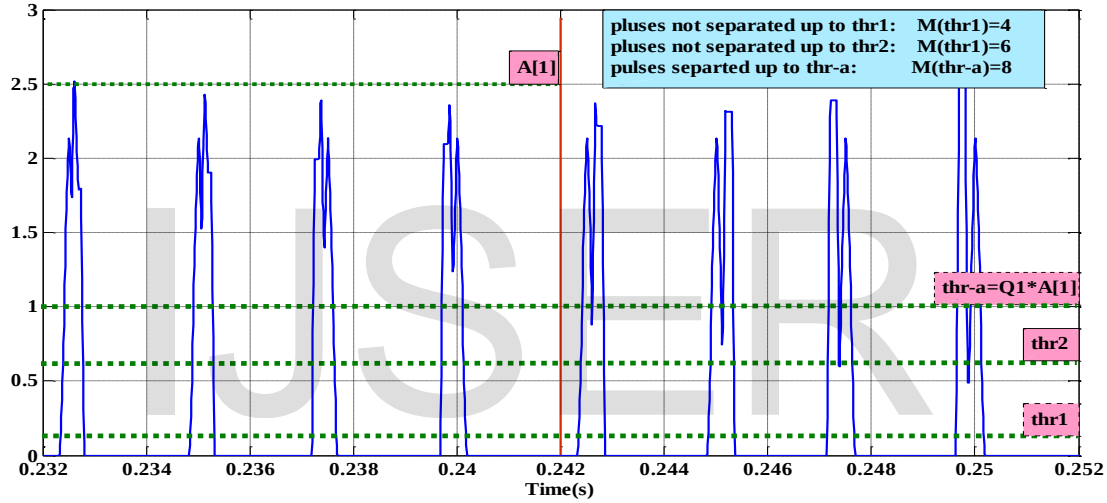

Fig.10. Pulses detection using an adaptive threshold.

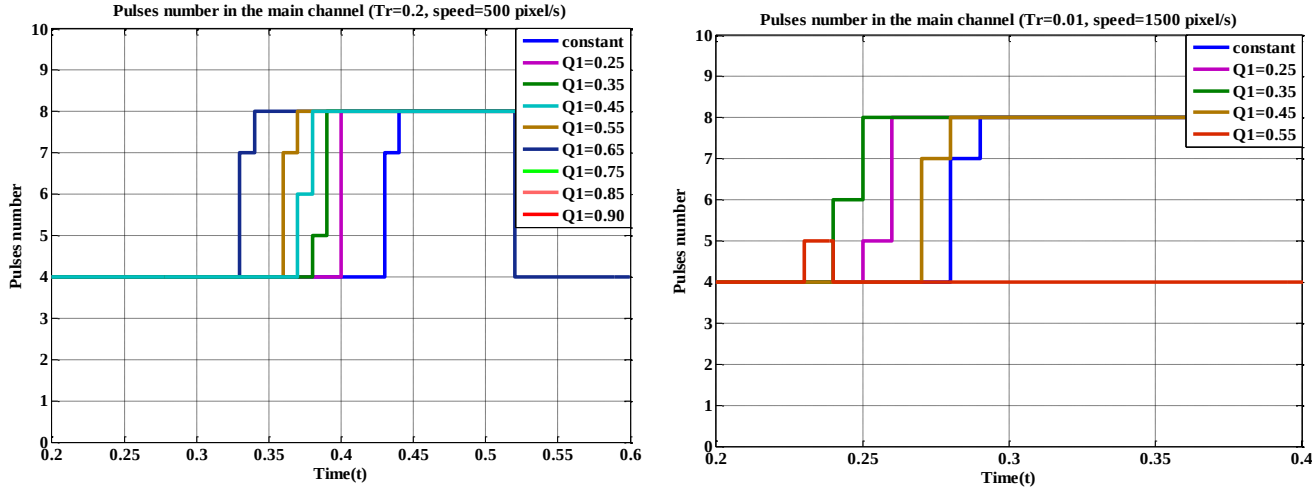

Fig 11 The pulses number for a Flare (Tlanuch=0.2s, Trise=0.25s, Tf=3.5s, Tb=4, Tmax=2000k, Tmin=850k) with several values of the parameter Q1 in the main channel: (a) Tr=0.2 , speed 500 pixel/s (b) Tr=0.01 , speed 1500 pixel/s.

IJSER © 2013
http://www.ijser.org

TABLE 2

THE REQUIRED TIME FOR DETECTION (TREQ (S)) USING (M(TH-A)>4) CONDITION FOR SEVERAL TR AND Q1WITH SPPED=500 PIXEL/S.

Q1	Tr	0.01	0.1	0.2
constant		0.23	0.24	0.23
0.25		0.17	0.17	0.20
0.35		0.11	0.16	0.19
0.45		0.19	0.14	0.17
0.55		none	0.14	0.16
0.65			none	0.13

TABLE 3

THE REQUIRED TIME FOR DETECTION (TREQ (S)) USING (M(TH-A)>4) CONDITION FOR SEVERAL TR AND Q1WITH SPPED=1500 PIXEL/S.

Q1	Tr	0.01	0.1	0.2
constant		0.08	0.08	0.08
0.25		0.06	0.07	0.07
0.35		0.05	0.07	0.07
0.45		0.05	0.07	0.06
0.55		0.05	0.0.6	0.09
0.65		None	0.06	0.11

TABLE 4

THE REQUIRED TIME FOR DETECTION (TREQ (S)) USING (M(TH-A)>4) CONDITION FOR SEVERAL TR AND SPEEDS.

Speed (pixel/s)	Tr	0.01	0.05	0.1	0.2	0.3
500		0.11	0.14	0.16	0.19	0.19
1000		0.06	0.09	0.10	0.10	0.10
1500		0.05	0.07	0.07	0.07	0.07
2000		0.04	0.05	0.05	0.05	0.07

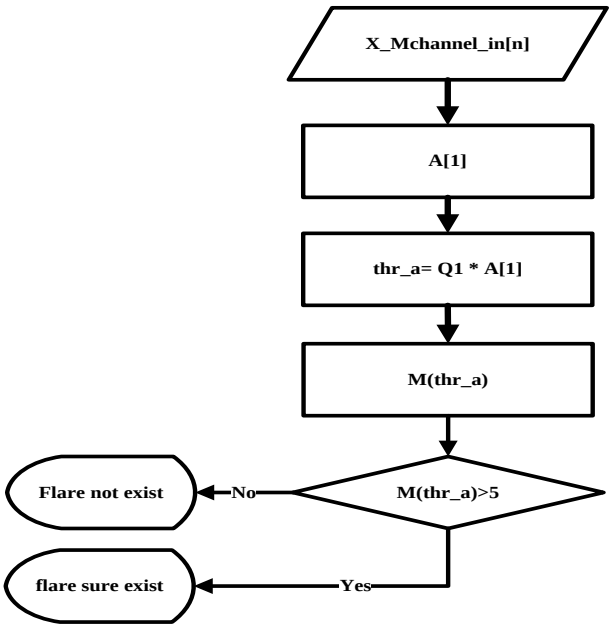

Fig.12. the flowchart of the flare detection using M(thr_a).

6 DETECTION OF AN ACTIVE JAMMER

In the first stage, detecting the active jammer is the same process of the flare, but after that it has to decide which the kind of jammer the detected jammer is. The idea is that, the flare separates away from the target with the time, but the active jammer does not. So it is enough to note the separation of the two first pulses, if this separation still fix that means the jammer is active; otherwise, the jammer is a flare [6-8].

As a result, the existence of an active jammer will produce four groups of pulses; each group consists of several pulses and can be procced to find the real pulse of each group. While the existence of a flare will produce two groups of pulses, each one consistes of four pulses, one for the flare and the other for the real target; one of these group will be canceled and the other will be considered as the real one.

7 COMPARISON OF THE FLARE DETECTION METHODS.

The more effective and robust method for detecting the flare existence of appearance is the method which can exploit the movement and the temperature of the flare to detect it in both the first phase and the second one one. The first phase is the duration between the flare launch and the instant when the pulses of the flare and those of the target are separated in the information signal, and the second is the phase after this separation. Some methods, like (PW, RPmax, Rmax) as shown in table 17, cannot detect in the second phase which means the flare detection can be missed and the existence detection is not possible. Other methods, like (PP, ARM, ARS, RPmax, RPmin, dRP, Rmax, MM, MS), cannot detect in the first phase, totally or limitedly, which means losing the detection or takes long time for detection.

The methods which can detect in both the phases, as shown in table 17, are (AR, Rmin, MA). AR depends mainly on the temperature profile and the main channel amplitude profile which makes it under the possible influence of the fluctuations or the perturbations on the main channel signals resulting from a possible unstable navigation or a strong background. Also, Rmin cannot take into account the target with high temperature.

On the other hand, MA method exploits the movement and the temperature of the flare which gives the ability to detect in both the phases without the influence of any high noise, perturbations and fluctuations on the main channel signal as the threshold is adaptive. In addition to that it doesn't influence of possible high temperature of the real target as it depends on the spatial separation of the thermal sources in the FOV. Also, MA method takes minimum required time for detecting and it can detect the existence as effectively as the appearance. Finally MA method is an effective method in comparison with other methods of flare detection.

IJSER © 2013
http://www.ijser.org

TABLE 5

COMPARISON OF THE FLARE DETECTION METHODS

Detecting parameter	First phase	Second phase	Using movement effect	Using temperature profile
Pluses width (PW)	yes	no	yes	no
Pulses position (PP)	no	yes	yes	no
Amplitude rate_main (ARM)	limited	yes	little	yes
Amplitude rate_secondary (ARS)	limited	yes	little	yes
RPmax	limited	no	yes	yes
RPmin	limited	yes	yes	yes
dRP	no	yes	yes	no
Rmax	no	no	no	no
Rmin	yes	yes	no	yes
dR	yes	yes	no	yes
Pulses number M_main (MM)	no	yes	yes	no
Pulses number M-secondary (MS)	no	yes	yes	no
M(thr_a) (MA)	yes	yes	yes	yes

- *RPmax= max{ RP[i]=: 1≤i ≤Number of pulses }the max ratio of the two channel of each pulses in the spinning period.*
- *RPmin= min{ RP[i]: 1≤i ≤Number of pulses }the min ratio of the two channel of each pulses in the spinning period.*
- *Rmax = max{ R[n]: n is the spin period } the max ratio of the two channel in the spinning period.*
- *Rmin = min{ R[n]: n is the spin period } the min ratio of the two channel in the spinning period.*
- *dRmax= Rmax- Rmin, dRPmax= RPmax- RPmin.*

TABLE 6

COMPARISON OF THE EFFECTIVE FLARE DETECTION METHODS

Detecting parameter	First phase	Second phase	Using movement effect	Using temperature profile
Amplitude rate_main	yes	yes	little	yes
Rmin	yes	yes	no	yes
M(thr_a)	yes	yes	yes	yes

8 CONCLUSION.

Designing and implementing effective IRCCM needs good simulation tools and good understanding of the signals generated from the seeker as a result of the existence of a target in the FOV. And one of the important steps is the flare detection. In this work, the flare is modeled by modeling its movement in the FOV and modeling its temperature profile. This model takes 6 variable inputs for the flare temperature and 2 for its positions; a as result a large scanning of the possible flare scenarios could be covered. Several methods are used; some depend on the main channel amplitude or the secondary channel amplitude like (ARM, ARS). Others used the two color characteristics of the seeker like (RPmax, RPmin, dRP) group and (Rmax,Rmin, dR) group. The third type of methods used the reticle structure characteristics like (M, MA). A comparison is discussed between these methods and the effective methods are stated. Finally, the more effective method, which is the detection using the pulses number in one spin period relatively to an adaptive threshold (MA), is found and its capabilities is stated over the wide spectrum of the possible cases of the flares; that included the required time of detecting, detection in both the first phase and the second one, detecting high temperature real target, and overcoming the possible perturbations on the main channel.

REFERENCES

[1] G. Gerson and A. K. Rue, "Tracking Systems," Chap. 22 in The Infrared Handbook, G. J. Zissis and W. L. Wolfe, Eds., RIM, Ann Arbor, MI(1985).

[2] K. Seyrafi and S. A. Hovanessian, Chap. 7 in Introduction to Electooptical Imaging and Tracking Systems, pp. 193–220, Artech House,Norwood, MA(1993).

[3] R. Legault, "Reticle and Image Analyses," Chap. 17 in The Infrared Handbook, revised ed., W. L. Wolfe and G. J. Zissis, Eds., pp. 17-1–17-49, Environmental Research Institute of Michigan, Ann Arbor, MI(1985).

[4] J. S. Accetta and D. L. Shymaker, Eds., "The Infrared & Electro-Optical Systems Handbook", SPIE Press (1993).

[5] J. S. Oh, K. S. Doo, S. G. Jahng, and J. S. Choi, "A New Counter-Countermeasure Algorithm for Two-Color Infrared Seekers," Optical Engineering, vol. 40, No. 8 (2001).

[6] S Y AlchekhYasin, A R Yrfanean, M R Mosavi and A Mohammadi, "Modeling and Simulation of the Active Jammer Effect in the Crossed Array Detectors Infrared Seeker," International Journal of Computer Applications 72(4):15-22, June 2013.

IJSER © 2013
http://www.ijser.org

[7] A R Yrfanean, M R Mosavi, A Mohammadi and Alchekh S Y Yasin, "Improving the Target Position Detection in the Crossed Array Detectors Seeker by Categorizing the FOV up to the Pulses Distribution," International Journal of Computer Applications72(4):28-36, June 2013.

[8] Z. W. Chao and J. L. Chu, "General Analysis of Frequency-Modulation Reticles," Opt. Eng. 27, 440—442 (1988).

[9] M. A. Porras, J. Alda, and E. Bernabeu, "Amplitude-Modulated and Frequency-Modulated Reticle Responses of Gaussian Beams," Optical Engineering, Vol. 30, No. 12 (1991).

[10] R. G. Driggers, C. E. Halford, and G. D. Boreman, "Use of Spatial Light Modulators in Frequency Modulation Reticle Trackers," Optical Engineering. Vol. 29, No. 11, pp. 1398-1403 (1990).

[11] W. Haifeng, L. Zhi, Z, Qing, and S. Xinzhi, "A Double Infrared Image Processing System Using Rosette Scanning," Proceeding. SPIE, Vol. 2894, pp. 2-10 (1996).

[12] S. G. Jahng, H. K. Hong, S. H. Han, and J. S. Choi, "Dynamic Simulation of The Rosette Scanning Infrared Seeker and an IRCCM using The Moment Technique," Opt. Eng. 38(5), 921–928 (1999).

[13] J. S. Oh, K. S. Doo, S. G. Jahng, D. S. Seo, and J. S. Choi, "Novel Adaptive Digital Signal Processing Algorithm for a Stationary Reticle Seeker," Optical Engineering, Vol. 39, No. 1 0, pp. 2797-2803, 2000.

[14] "Development of an IR Signature Model," [Online]. available:https://dspace.lib.cranfield.ac.uk/bitstream/.../CHAPTER_6_july26.pdf.

[15] M. R. Mosavi, M. Asadpour, and R. Kalili,"Comparing Performance of Two Infrared Anti-Jamming Methods using Fuzzy System and Neural Network," 2007 Congress on Intelligent and Fuzzy Systems, Ferdowsi University of Mashhad, Iran (2007).

[16] M. R. Mosavi, M. Asadpour, and H. A. Amerim,"Design and Simulation of an Infrared Jammer Source for an Infrared Seeker," IEEE Conference on Signal Processing, Communications, and Networking, India (2008)

IJSER © 2013
http://www.ijser.org